Received: Added at production | Revised: Added at production | Accepted: Added at production

DOI: xxx/xxxx

ARTICLE TYPE

Observer-based predictor for a SIR model with delays: An optimal-control case study

Fernando Castaños | Sabine Mondié*

[1]Department of Automatic Control, Cinvestav-IPN, Mexico City, Mexico

Correspondence
*Sabine Mondié. Email: smondie@ctrl.cinvestav.mx

Present Address
Av. Instituto Politécnico Nacional 2508, Col. San Pedro Zacatenco, Gustavo A. Madero, C.P. 07360, Ciudad de México, México

Summary

We propose an observer for a SIR epidemic model. The observer is then uplifted into a predictor to compensate for time delays in the input and the output. Tuning criteria are given for tuning gains of the predictor, while the estimation-error stability is ensured using Lyapunov-Krasovskii functionals. The predictor's performance is first evaluated in combination with a time-optimal control. It is shown that the predictor nearly recovers the performance level of the delay-free system. Finally, the predictor is evaluated using real data from a covid epidemic.

KEYWORDS:
Input-delay systems, predictor, optimal-control, nonlinear systems, epidemiological models

1 | INTRODUCTION

Epidemics are a good example of how reality challenges researchers, offering the opportunity to show the strength of existing techniques and develop new ones in fields as varied as medicine, biology, computational sciences, and mathematical system theory.

Epidemiological models have been primarily used for prediction purposes, while mitigation policies are usually decided based on exhaustive simulations. From the perspective of control theory, an epidemic is viewed as a dynamical system with controlled variables. Its model is an instrument for designing a control action that will achieve the desired outcome. Depending on the context, different assumptions on the model and other control objectives can be formulated. Most works focus on vaccination or treatment policies, with the goals expressed in an optimal-control framework [1]. In the context of the current covid pandemic, with vaccines scarce or unavailable in many countries, intervention policies based on social distancing measures remain the core containment tool. Considering the dramatic effect that extended lockdowns have on people and countries economies, a minimum-time control using social distancing measures and considering hospital capacity restrictions was recently presented for the SIR model [2].

The SIR model, which we also consider in this paper, is arguably the simplest epidemiological model. However, it already exhibits many of the nonlinear characteristics that are present in more elaborate models. We make the model more realistic by adding features such as inaccurate and partial state measurements, and input and measurement delays. In recent months, delays in measurements and policy implementation have proved to be critical in the success or failure of government strategies. The former correspond to the time taken for the tests to be carried out, processed, verified, and made available in centralized databases. The latter correspond to the time it takes the population to adopt restrictions such as quarantine, social distancing habits, and mask use.

Due to the prevalence of delays in the feedback loops of control systems and the associated detrimental effects on performance, input and output delays have received sustained attention in the past decades. Some early strategies for compensating the delays

[0]**Abbreviations:** SIR, susceptible-infectious-recovered; ICU, intensive care unit; LMI, linear matrix inequality

are the Smith controller[3], the transformation-based reduction approach[4], and the time-domain predictor-based designs[5]. Based on present state information, predictors based on Cauchy's formula provide the state ahead of time[6]. They were formally shown to ensure closed-loop stability[7], but their practical implementation reveals instabilities due to neutral phenomena related to the integrals' discretization in Cauchy's formula. These issues inspired new proposals such as filtered predictors[8,9], and truncated predictors[10]. If the present state is not entirely measurable, it can be replaced by an estimation, provided that the system is observable[11].

A recent approach to the compensation of delays consists of modifying an observer to predict future states. It was first introduced for the case of linear systems with full-state information[12] and later extended to the partial information scenario[13]. This approach, called observer-predictor, is inspired on the proposal of chain observers for systems with delayed measurements studied in a differential geometry framework[14,15]. It also suffers from some drawbacks: It loses the exact nature of predictions obtained with Cauchy's formula and requires the inclusion of extra sub-predictors designed via LMI techniques. However, it has significant advantages: The observer has the same structure as the system (modulo an output injection term), thus avoiding integrals in the prediction formulae. Also, it is readily applicable to the case of partial state information in observable systems, especially when observers are readily available. Systems with state delays[16] or nonlinear systems[17] can be modified easily to successfully compensate for input or output delays.

To tackle the complexity due to partial state availability, delay, and measurement errors, we resort to a wide array of tools available to specialists in the field of control of dynamical systems. For the control, we use a recent optimal law[2]. The objective is not to steer the epidemics towards a desired equilibrium. Instead, the aim is to track an optimal trajectory. As a result, the dynamics for the estimation error are time-varying and time-delayed. The stability of such dynamics is addressed from both the perspective of classical frequency-domain quasipolynomial analysis[18,19], and from the perspective of time-domain Lyapunov-Krasowskii analysis[20,21]. In particular, the system's time-varying nature is taken into account by embedding the system into a model with polytopic uncertainty[22,23].

It is worthy of mention that the design of observers for systems with output delay have received a sustained attention in past and recent years. See, for example, the approach based on differential geometry[15], on extended pseudo linearization combined with state Riccati equations[24], on the Hamiltonian function[25], and the references therein.

In Section 2, we introduce the SIR model and discuss the issues we want to overcome. An *ad hoc* change of variable allows designing an observer addressing incomplete state information for the delay-free system. In Section 3, this observer is developed into an observer-based predictor for the system with input and output delays. The next two sections are devoted to tuning the observer: A simple criterion to tune the observer gains is given in Section 4, and conditions for the stability of the prediction error dynamics are given in Section 5. The impact of measurement errors is discussed in Section 6. We show the validity of our approach by discussing a SIR case study along with the paper, which is of interest in its own right, and which is verified against real data in Section 7. We conclude with some remarks.

Allow us to recall some standard notation used in the literature of time-delay systems.

Notation.

$\boldsymbol{PC}([-\eta, 0], \mathbb{R}^n)$ is the set of piece-wise continuous functions defined on the interval $[-\eta, 0]$. Consider a time-delay differential equation

$$\dot{\varepsilon}(\tau) = f(\tau, \varepsilon(\tau), \varepsilon(\tau - \eta(\tau))) \, . \tag{1}$$

The time-varying delay, $\eta(\tau)$, is bounded by $0 < \eta(\tau) \leq \bar{\eta}$. Given an initial function $\varphi \in \boldsymbol{PC}([-\eta(0), 0], \mathbb{R}^n)$ the solution is denoted by $\varepsilon(\tau, \varphi)$. The restriction of $\varepsilon(\tau, \varphi)$ on the interval $[\tau - \eta(\tau), \tau]$ is denoted by

$$\varepsilon_\tau(\varphi) : \theta \mapsto \varepsilon(\tau + \theta, \varphi) \, , \quad \theta \in [-\eta(\tau), 0] \, .$$

We will make use of the *trivial function* $0_{\bar{\eta}} : \theta \mapsto 0$, $\theta \in [-\bar{\eta}, 0]$. We use the Euclidean norm $\| \cdot \|$ for vectors and the corresponding induced norm for matrices. For $\varphi \in \boldsymbol{PC}([-\eta, 0], \mathbb{R}^n)$ we use the norm

$$\|\varphi\|_\eta = \sup_{\theta \in [-\eta, 0]} \|\varphi(\theta)\| \, .$$

The notation $Q > 0$ means that the symmetric matrix Q is positive definite.

2 | PROBLEM STATEMENT

We consider a state-space SIR model

$$\begin{aligned}\frac{\mathrm{d}}{\mathrm{d}t}S(t) &= -\beta(t-h_1)S(t)I(t)\\ \frac{\mathrm{d}}{\mathrm{d}t}I(t) &= (\beta(t-h_1)S(t)-\gamma)I(t)\\ y(t) &= I(t-h_2)\end{aligned}.$$

Here, $S > 0$, $I > 0$ denote the susceptible and the infected, respectively. The model is normalized, hence $S + I \leq 1$. The transmission rate, $\beta \in [\beta_{\min}, \beta_{\max}]$ with $\beta_{\max} > \beta_{\min} > 0$, can be controlled by applying social distancing measures, but such measures take effect h_1 units of time later. The only information available at time t is the number of infected people at time $t - h_2$. The recovery/death rate, $\gamma > 0$, and the time delays, h_1, h_2, are assumed to be known.

There are of course more sophisticated models. It is possible to include exposed individuals (infected but not infectious), to distinguish between symptomatic and asymptomatic, dead and recovered, etc. However, for epidemics the parameters of which have large levels of uncertainty, such as covid-19, a simple model with fewer parameters is preferable, as long as it is able to reproduce the main features of the epidemics (hospital saturation, lock-down effects, herd immunity, and so forth). A simpler model is also preferable when the objective is to devise decision strategies, rather that simulating long-term behavior.

Using only the history of y, we wish to produce predictions $\hat{S}, \hat{I}$ such that

$$\lim_{t\to\infty}(\hat{S}(t) - S(t+h_1), \hat{I}(t) - I(t+h_1)) = 0\ .$$

Our motivation is that, if we have a feedback $\beta^*(S, I)$ that is known to perform correctly on the system without delays, we can set $\beta = \beta^*(\hat{S}, \hat{I})$ and expect to recover a similar performance[1].

For concreteness, we consider the optimal-time control strategy described by Angulo *et al*[2]. For the SIR model, the basic (unmitigated) reproduction number is computed as $R_0 = \beta_{\max}/\gamma$, while the controlled (mitigated) reproduction number is $R_c = \beta_{\min}/\gamma$. Suppose that the health system capacity of a given city is limited to $I_{\max}$ infected people. The strategy that ensures $I(t) \leq I_{\max}$ and achieves herd immunity in a minimal time is

$$\beta^\star(S, I) = \begin{cases}\beta_{\max} & \text{if } I < \Phi(S)\\ \beta_{\min} & \text{otherwise}\end{cases} \tag{2}$$

with

$$\Phi(S) = \begin{cases} I_{\max} + \frac{1}{R_c}\ln\left(\frac{S}{S^\star}\right) - (S - S^\star) & \text{if } S^\star \leq S \leq 1\\ I_{\max} & \text{if } 0 \leq S \leq S^\star\end{cases}$$

and

$$S^\star = \min\left\{\frac{1}{R_c}, 1\right\}\ .$$

We consider a recovery rate $\gamma = 1/7$ with time units given in days[2]. For illustration purposes, we consider the case of Mexico City. The number of ICU beds is such that $I_{\max} = 12.63 \times 10^{-3}$ (see[2]). We take the reproduction numbers as $R_0 = 1.7$ and $R_c = 1.1$[2]. This gives

$$\beta_{\max} = 1.7/7 \quad \text{and} \quad \beta_{\min} = 1.1/7\ .$$

The optimal response, achieved with full state-feedback in the absence of delays, is shown in Fig. 1. The optimal strategy is to allow the epidemic to run free until it reaches the sliding curve $I = \Phi(S)$. The state is then driven along this curve towards the region of herd immunity (gray rectangle) where the intervention finally stops. For implementation purposes, one can replace the discontinuous action (2) with a continuous approximation, such as Yoshida's[26, Ch.32].

Suppose now that there is a delay of $h_1 = 3$ days in the control action. Figure 2 confirms the appearance of the so-called *chattering* effect, which should not be surprising given the discontinuous nature of (2). We can expect the performance of the closed-loop system to deteriorate even further when only the number of infected people is available for measurement, and when such measurements are also subject to important delays. The objective of the predictor, developed in the following section, is to mitigate these unfavorable effects.

[1] The full analysis would have to be performed, of course.
[2] Indeed, this is how we will perform all simulations.

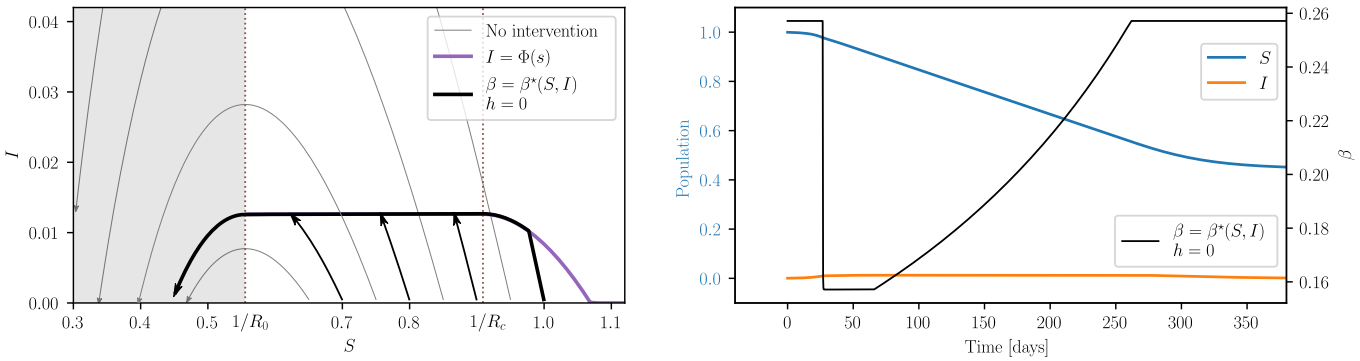

FIGURE 1 Phase-plane of the model under the optimal feedback law (2) (left). The trajectory with thick line is depicted on the right (blue and orange, scale shown on the left axis). The control action is also included (black, scale shown on the right axis).

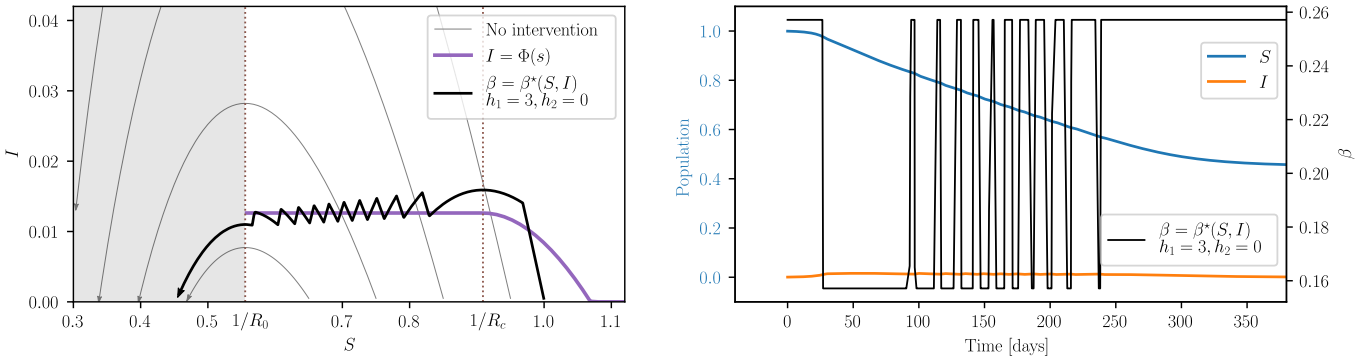

FIGURE 2 Trajectory corresponding to the feedback law (2) subject to a delay of $h_1 = 3$ days. The trajectory ultimately results in chattering.

3 | OBSERVER-BASED PREDICTOR

To attain our objective we follow the approach in which an observer for the delay-free system is constructed in a first step, and then developed into a predictor in a second one [12,16,17].

3.1 | Delay-free observer

We begin by making the temporary assumption $h_1 = h_2 = 0$. Note that, by setting $x_1 = \ln(y)$ and $x_2 = S$, we obtain the model

$$\begin{aligned}\frac{\mathrm{d}}{\mathrm{d}t}x_1(t) &= \beta(t)x_2(t) - \gamma\\ \frac{\mathrm{d}}{\mathrm{d}t}x_2(t) &= \beta(t)\rho(x(t))\end{aligned}$$

with $\rho(x) = -x_2 \mathrm{e}^{x_1}$. The main advantage over the original model is that the first equation is affine in the state. We can then write the simple observer

$$\begin{aligned}\frac{\mathrm{d}}{\mathrm{d}t}\tilde{x}_1(t) &= \beta(t)\left(\tilde{x}_2(t) + \alpha_1(x_1(t) - \tilde{x}_1(t))\right) - \gamma\\ \frac{\mathrm{d}}{\mathrm{d}t}\tilde{x}_2(t) &= \beta(t)\left(\rho(\tilde{x}(t)) + \alpha_2(x_1(t) - \tilde{x}_1(t))\right)\end{aligned},$$

where α_1, α_2 will be defined below (Proposition 1). Consider the error $\epsilon = x - \tilde{x}$. By using the expansion

$$\rho(\tilde{x}) = \rho(x) + \left(-x_2\mathrm{e}^{x_1} \;\; -\mathrm{e}^{x_1}\right)\epsilon + \mathcal{O}(\|\epsilon\|^2)\,,$$

we can write the error dynamics as

$$\frac{\mathrm{d}}{\mathrm{d}t}\begin{pmatrix}\epsilon_1(t)\\ \epsilon_2(t)\end{pmatrix} = \beta(t)A(t)\begin{pmatrix}\epsilon_1(t)\\ \epsilon_2(t)\end{pmatrix} + \mathcal{O}(\|\epsilon(t)\|^2) \tag{3}$$

with

$$A(t) = \begin{pmatrix}-\alpha_1 & 1\\ -\alpha_2 - S(t)I(t) & -I(t)\end{pmatrix} .$$

Note that, since we are linearizing the estimation error around a trajectory (rather than an equilibrium), the linearized system is time-varying. Fortunately, we can ensure its stability with a simple quadratic Lyapunov function.

Proposition 1. Set

$$\alpha_2 > \frac{\alpha_1^2+1}{4\sqrt{2}\alpha_1 - 1} , \quad \alpha_1 > \frac{1}{4\sqrt{2}} \tag{4}$$

Then (3) is locally quadratically stable[3].

Proof. Consider the candidate Lyapunov function $V(\epsilon) = \epsilon^\top P\epsilon$ with $P = P^\top > 0$ the solution of the Lyapunov equation

$$P\begin{pmatrix}-\alpha_1 & 1\\ -\alpha_2 & 0\end{pmatrix} + \begin{pmatrix}-\alpha_1 & -\alpha_2\\ 1 & 0\end{pmatrix}P = -\begin{pmatrix}1 & 0\\ 0 & 1\end{pmatrix} ,$$

that is,

$$P = \frac{1}{2\alpha_1\alpha_2}\begin{pmatrix}\alpha_2^2+\alpha_2 & -\alpha_1\alpha_2\\ -\alpha_1\alpha_2 & \alpha_1^2+\alpha_2+1\end{pmatrix} . \tag{5}$$

The time-derivative of V along the trajectories of (3) is

$$\dot{V}(\epsilon(t)) = -\frac{\beta(t)}{2\alpha_1\alpha_2}\epsilon^\top(t)W(S(t),I(t))\epsilon(t) + \mathcal{O}(\|\epsilon(t)\|^3)$$

with

$$W(S,I) = \begin{pmatrix}2(1-SI)\alpha_1\alpha_2 & (\alpha_1^2+\alpha_2+1)SI - \alpha_1\alpha_2 I\\ (\alpha_1^2+\alpha_2+1)SI - \alpha_1\alpha_2 I & 2\left(\alpha_1\alpha_2 + (\alpha_1^2+\alpha_2+1)I\right)\end{pmatrix} . \tag{6}$$

The restrictions $(S,I)\in[0,1]^2$, $S+I\leq 1$ imply that $SI\leq 1/4$, so the first leading principal minor of $W(S,I)$, $2(1-SI)\alpha_1\alpha_2$, is strictly positive. Regarding the second leading principal minor, we have

$$|W(S,I)| = \alpha_1^2\alpha_2^2\left(4(1-SI)-I^2\right) + \alpha_1\alpha_2(\alpha_1^2+\alpha_2+1)(4-2SI)I - (\alpha_1^2+\alpha_2+1)^2S^2I^2 .$$

Using again $SI\leq 1/4$ we obtain the bound

$$|W(S,I)| \geq 2\alpha_1^2\alpha_2^2 - \frac{1}{16}(\alpha_1^2+\alpha_2+1)^2 .$$

Finally, the condition (4) ensures that $|W(S,I)|>0$, so that V is indeed a Lyapunov function. □

In the original coordinates, the observer takes the form

$$\begin{aligned}\frac{\mathrm{d}}{\mathrm{d}t}\tilde{S}(t) &= -\beta(t)\left(\tilde{S}(t)\tilde{I}(t) - \alpha_2\ln\left(\frac{y(t)}{\tilde{I}(t)}\right)\right)\\ \frac{\mathrm{d}}{\mathrm{d}t}\tilde{I}(t) &= \left(\beta(t)\tilde{S}(t) - \gamma + \beta(t)\alpha_1\ln\left(\frac{y(t)}{\tilde{I}(t)}\right)\right)\tilde{I}(t)\end{aligned} . \tag{7}$$

A simulation of the observer's performance is shown in Fig. 3. The observer gains, $\alpha^\top = \begin{pmatrix}\alpha_1 & \alpha_2\end{pmatrix} = \begin{pmatrix}4 & 1\end{pmatrix}$ were chosen to satisfy (4). At first, the incidence of infection exceeds $I_{\max}$ by about 12 %, but then the epidemics behave as desired.

Consider again the input delay $h_1 = 3$ days, and suppose now there is a measurement delay of $h_2 = 7$ days[27]. The combined effect of both delays is disastrous. As illustrated in Fig. 4, the hospital capacity is exceeded by more than 200 %. This motivates the design of the predictor presented in the sequel.

[3] Recall that (3) is quadratically stable if there is a common quadratic Lyapunov function for all possible $A(t)$ [22, Ch. 5].

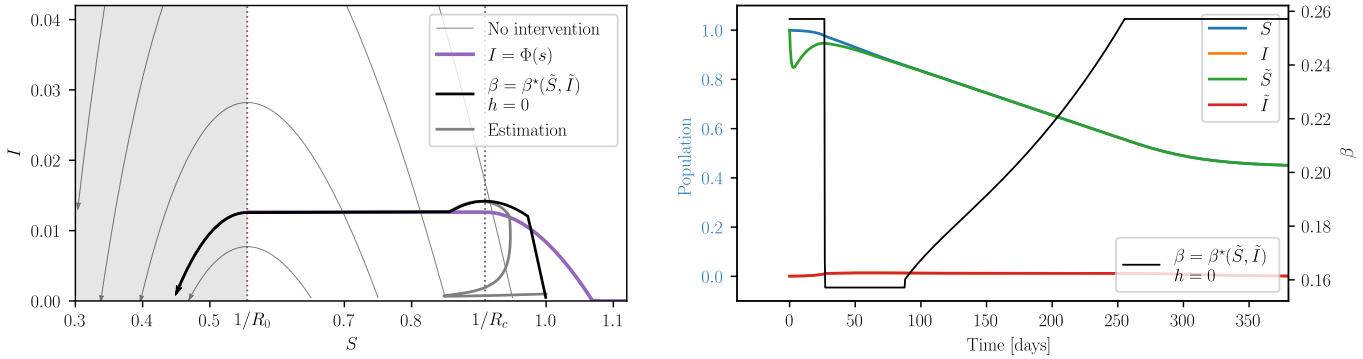

FIGURE 3 True and estimated trajectories under the feedback law $\beta = \beta^\star(\tilde{S}, \tilde{I})$, with no delays.

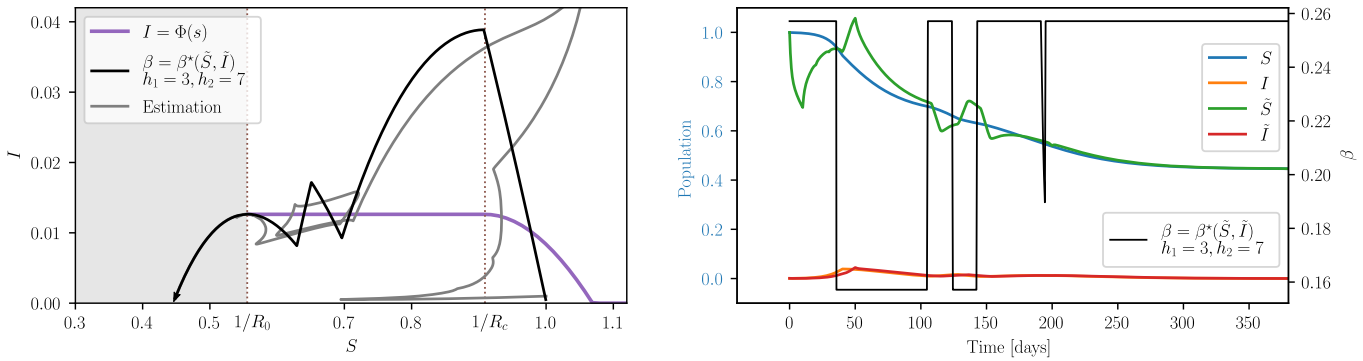

FIGURE 4 True and estimated trajectories under the feedback law $\beta = \beta^\star(\tilde{S}, \tilde{I})$ with $h_1 = 3$ and $h_2 = 7$ days.

3.2 | Predictor

Let us rewrite the observer in the original coordinates and remove the zero-delays assumption. This gives the predictor

$$\begin{aligned}\frac{\mathrm{d}}{\mathrm{d}t}\hat{S}(t) &= -\beta(t)\left(\hat{S}(t)\hat{I}(t) - \alpha_2 \ln\left(\frac{y(t)}{\hat{I}(t-h)}\right)\right)\\ \frac{\mathrm{d}}{\mathrm{d}t}\hat{I}(t) &= \left(\beta(t)\hat{S}(t) - \gamma + \beta(t)\alpha_1 \ln\left(\frac{y(t)}{\hat{I}(t-h)}\right)\right)\hat{I}(t)\end{aligned} \tag{8}$$

with $h = h_1 + h_2$. Considering that $y(t) = I(t - h_2)$, the error variables

$$\begin{aligned}\epsilon_1(t) &= \ln\left(\frac{I(t)}{\hat{I}(t-h_1)}\right)\\ \epsilon_2(t) &= S(t) - \hat{S}(t-h_1)\end{aligned} \tag{9}$$

evolve according to the dynamics

$$\begin{aligned}\frac{\mathrm{d}}{\mathrm{d}t}\epsilon_1(t) &= \beta(t-h_1)\left(S(t) - \hat{S}(t-h_1) - \alpha_1 \ln\left(\frac{I(t-h)}{\hat{I}(t-h-h_1)}\right)\right)\\ \frac{\mathrm{d}}{\mathrm{d}t}\epsilon_2(t) &= \beta(t-h_1)\left(-\alpha_2 \ln\left(\frac{I(t-h)}{\hat{I}(t-h-h_1)}\right) + \hat{S}(t-h_1)\hat{I}(t-h_1) - S(t)I(t)\right)\end{aligned}. \tag{10}$$

Since $\hat{I}(t-h_1) = \mathrm{e}^{-\epsilon_1(t)}I(t)$ and $\hat{S}(t-h_1) = S(t) - \epsilon_2(t)$, we have

$$\begin{aligned}\frac{\mathrm{d}}{\mathrm{d}t}\epsilon_1(t) &= \beta(t-h_1)\left(-\alpha_1\epsilon_1(t-h) + \epsilon_2(t)\right)\\ \frac{\mathrm{d}}{\mathrm{d}t}\epsilon_2(t) &= \beta(t-h_1)\left(-\alpha_2\epsilon_1(t-h) + \psi(S(t), I(t), \epsilon(t))\right)\end{aligned} \tag{11}$$

with

$$\psi(S, I, \epsilon) = ((S - \epsilon_2)\mathrm{e}^{-\epsilon_1} - S)I \ . \tag{12}$$

System (11) can be written in the general form

$$\frac{\mathrm{d}}{\mathrm{d}t}\epsilon(t) = \beta(t - h_1)\left[A_0(t)\epsilon(t) + A_1\epsilon(t - h) + G(t, \epsilon(t))\epsilon(t)\right] \tag{13}$$

where the matrices are defined by

$$A_0(t) = \begin{pmatrix} 0 & 1 \\ -S(t)I(t) & -I(t) \end{pmatrix} \ , \quad A_1 = \begin{pmatrix} -\alpha_1 & 0 \\ -\alpha_2 & 0 \end{pmatrix} \tag{14}$$

and

$$G(t, \epsilon) = \begin{pmatrix} 0 & 0 \\ G_{21}(t, \epsilon) & G_{22}(t, \epsilon) \end{pmatrix} = \mathcal{O}(\|\epsilon\|)$$

with

$$\begin{aligned} G_{21}(t, \epsilon) &= -S(t)I(t)\frac{\mathrm{e}^{-\epsilon_1} + \epsilon_1 - 1}{\epsilon_1} \\ G_{22}(t, \epsilon) &= -I(t)(\mathrm{e}^{-\epsilon_1} - 1) \end{aligned} \ . \tag{15}$$

Since β multiplies all the right-hand side of (13), we can do away with it by rescaling time, much in the spirit of perturbation theory [28, Ch. 10]. Define the new time-scale

$$\tau = g(t) = \int_0^t \beta(s - h_1)\mathrm{d}s \ .$$

Since β is strictly positive, g is strictly increasing, invertible and τ is indeed a time-scale. Let us define the new state

$$\varepsilon(\tau) = \epsilon(g^{-1}(\tau))$$

and note that, by the Inverse Function Theorem, we have

$$\frac{\mathrm{d}}{\mathrm{d}\tau}g^{-1}(\tau) = \left.\frac{1}{\frac{\mathrm{d}}{\mathrm{d}t}g(t)}\right|_{t=g^{-1}(\tau)} = \left.\frac{1}{\beta(t - h_1)}\right|_{t=g^{-1}(\tau)} \ . \tag{16}$$

Applying the chain rule and (16), we see that the new state evolves according to

$$\frac{\mathrm{d}}{\mathrm{d}\tau}\varepsilon(\tau) = \frac{1}{\beta(t - h_1)}\frac{\mathrm{d}}{\mathrm{d}t}\epsilon(t)\Big|_{t=g^{-1}(\tau)} \ ,$$

that is,

$$\dot{\varepsilon}(\tau) = B_0(\tau)\varepsilon(\tau) + B_1\varepsilon(\tau - \eta(\tau)) + H(\tau, \varepsilon(\tau))\varepsilon(\tau) \tag{17}$$

with

$$B_0(\tau) = A_0(g^{-1}(\tau)) \ , \quad B_1 = A_1 \ , \quad H(\tau, \varepsilon) = G(g^{-1}(\tau), \varepsilon)$$

and

$$\eta(\tau) = \tau - g(g^{-1}(\tau) - h) \ .$$

The last equation follows from the condition

$$\varepsilon(\tau - \eta(\tau)) = \varepsilon(g(g^{-1}(\tau) - h)) = \epsilon(g^{-1}(\tau) - h)) \ .$$

Observe that $\beta_{\min}h \leq \tau - g(t - h) = \int_{t-h}^{t} \beta(s - h_1)\mathrm{d}s \leq \beta_{\max}h$, so the time-varying delay is bounded by

$$\beta_{\min}h \leq \eta(\tau) \leq \beta_{\max}h \ .$$

For ease of reference, we will define

$$\bar{\eta} = \beta_{\max}h \ . \tag{18}$$

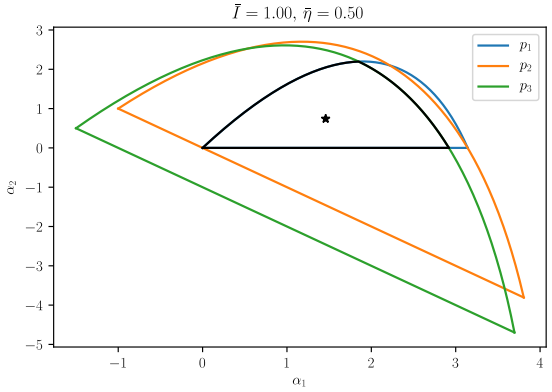

FIGURE 5 Stability/instability boundaries of the quasipolynomials (21) in the space of parameters (α_1, α_2) for $\bar{I} = 1$ and $\bar{\eta} = 0.5$. The boundary of the intersection of the three regions is depicted in black.

4 | TUNING THE PREDICTOR GAINS

There are two main difficulties in establishing the stability of (17): The time-varying nature of B_0, and the presence of the delayed state. The former difficulty will be addressed by formulating (17) in the framework of polytopic differential inclusions [22, Ch. 5]. In order to do so, we will focus on the state-space rectangle $[0, 1] \times [0, \bar{I}]$, where $I_{\max} \leq \bar{I} \leq 1$. When the state is restricted to such rectangle, B_0 varies within a fixed polytope of matrices, i.e.,

$$B_0(t) \in \mathrm{Co}\{C_1, C_2, C_3\}\ , \tag{19}$$

where

$$C_1 = \begin{pmatrix} 0 & 1 \\ 0 & 0 \end{pmatrix}\ , \quad C_2 = \begin{pmatrix} 0 & 1 \\ 0 & -\bar{I} \end{pmatrix}\ , \quad C_3 \begin{pmatrix} 0 & 1 \\ -\bar{I} & -\bar{I} \end{pmatrix} \tag{20}$$

and Co stands for convex closure, that is,

$$\mathrm{Co}\{C_1, C_2, C_3\} = \left\{ \sum_{i=1}^{3} c_i \cdot C_i \mid c_i \geq 0,\ \sum_{i=1}^{3} c_i = 1 \right\}\ .$$

An obvious necessary condition for the stability of the polytopic model (17)-(19) is the stability of its linearized vertices,

$$\dot{\varepsilon}(\tau) = C_i \varepsilon(\tau) + B_1 \varepsilon(\tau - \bar{\eta})\ , \quad i = 1, 2, 3.$$

The characteristic equations of the vertices are

$$\begin{aligned} p_1(s) &= s^2 + \left(s\alpha_1 + \alpha_2\right) \mathrm{e}^{-\bar{\eta}s} \\ p_2(s) &= s^2 + \left((s + \bar{I})\alpha_1 + \alpha_2\right) \mathrm{e}^{-\bar{\eta}s} + s\bar{I} \\ p_3(s) &= s^2 + \left((s + \bar{I})\alpha_1 + \alpha_2\right) \mathrm{e}^{-\bar{\eta}s} + (s + 1)\bar{I} \end{aligned}\ . \tag{21}$$

We will work out the stability/instability boundaries of these quasipolynomials in the space of parameters (α_1, α_2). According to the D-partition method [18], these boundaries correspond to roots crossing the imaginary axis of the complex plane. When the crossing root is real ($s = 0$), the boundaries are

$$\begin{aligned} p_1 &: \quad \alpha_2 = 0 \\ p_2 &: \quad \alpha_2 = -\alpha_1 \bar{I} \\ p_3 &: \quad \alpha_2 = -(\alpha_1 + 1)\bar{I}\ . \end{aligned}$$

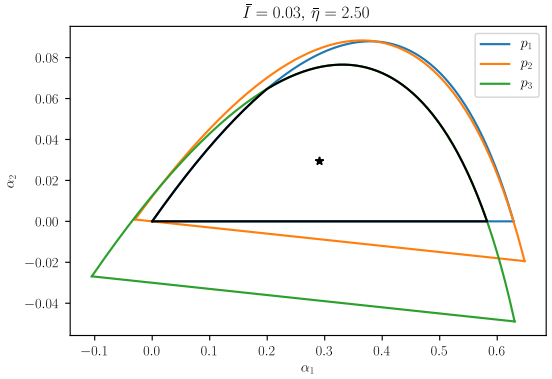

FIGURE 6 Stability/instability boundaries of the quasipolynomials (21) in the space of parameters (α_1, α_2) for $\bar{I} = 0.03$ and $\bar{\eta} = 2.5$. The boundary of the intersection of the three regions is depicted in black.

If a crossing root is imaginary ($s = j\omega$), the boundaries satisfy

$$p_1: \quad \begin{pmatrix} \omega\sin(\omega\bar{\eta}) & \cos(\omega\bar{\eta}) \\ \omega\cos(\omega\bar{\eta}) & -\sin(\omega\bar{\eta}) \end{pmatrix} \alpha = \begin{pmatrix} \omega^2 \\ 0 \end{pmatrix}$$

$$p_2: \quad \begin{pmatrix} \omega\sin(\omega\bar{\eta}) + \bar{I}\cos(\omega\bar{\eta}) & \cos(\omega\bar{\eta}) \\ \omega\cos(\omega\bar{\eta}) - \bar{I}\sin(\omega\bar{\eta}) & -\sin(\omega\bar{\eta}) \end{pmatrix} \alpha = \begin{pmatrix} \omega^2 \\ -\omega\bar{I} \end{pmatrix}$$

$$p_3: \quad \begin{pmatrix} \omega\sin(\omega\bar{\eta}) + \bar{I}\cos(\omega\bar{\eta}) & \cos(\omega\bar{\eta}) \\ \omega\cos(\omega\bar{\eta}) - \bar{I}\sin(\omega\bar{\eta}) & -\sin(\omega\bar{\eta}) \end{pmatrix} \alpha = \begin{pmatrix} \omega^2 - \bar{I} \\ -\omega\bar{I} \end{pmatrix}$$

The form and disposition of the stability regions depend on $\bar{\eta}$ and $\bar{I}$. Figure 5 shows their boundaries for a relatively small delay, $\bar{\eta} = 0.5$, and the largest incidence, $\bar{I} = 1$. Figure 6 shows the boundaries of the stability regions for a larger delay, $\bar{\eta} = 2.5$, but a smaller incidence, $\bar{I} = 0.03$. Since stability of the three vertices is a necessary condition for the stability of (17)-(19), we require α to be placed at the intersection of the three regions (boundaries drawn in black), for example, at an approximate centroid of the intersection (marked with $\star$).

5 | STABILITY OF THE PREDICTOR

Setting α as described in the previous section, i.e., at the intersection of the stability regions, only ensures that a necessary condition for stability is satisfied. We will now exploit the polytopic nature of (3) and the fact that stabilty is ensured by the existence of a Lyapunov-Krasowskii functional that is common to all the vertices of the polytope.

We will begin by summarizing a general assertion from the book by Fridman[21].

Lemma 1. Consider the candidate Lyapunov-Krasowskii functional

$$V(\varepsilon_\tau) = \varepsilon^\top(\tau)P\varepsilon(\tau) + \int_{\tau-\bar{\eta}}^{\tau} \varepsilon^\top(s)S\varepsilon(s)\mathrm{d}s + \bar{\eta}\int_{-\bar{\eta}}^{0}\int_{\tau+\theta}^{\tau} \dot{\varepsilon}^\top(s)R\dot{\varepsilon}(s)\mathrm{d}s\mathrm{d}\theta \tag{22}$$

with $P > 0$, $R \geq 0$, $S \geq 0$ and $\bar{\eta} \geq 0$. Define

$$E(\tau) = \left(\varepsilon(\tau)\ \dot{\varepsilon}(\tau)\ \varepsilon(\tau-\bar{\eta})\ \varepsilon(\tau-\eta(\tau))\right)^\top .$$

The time derivative of V satisfies

$$\dot{V}(\varepsilon_\tau) \leq E(\tau)^\top \begin{pmatrix} S-R & P & 0 & R \\ \star & \bar{\eta}^2 R & 0 & 0 \\ \star & \star & -(S+R) & 0 \\ \star & \star & \star & -2R \end{pmatrix} E(\tau)\,, \tag{23}$$

where the terms $\star$ are such that the overall matrix is symmetric.

The lemma is easily proved by differentiating V and applying Jensen's lemma [21, Ch. 3].

Theorem 1. Let

$$Q(C;P,R,S,P_2,P_3)=\begin{pmatrix} C^\top P_2+P_2^\top C+S-R & P-P_2^\top+C^\top P_3 & 0 & P_2^\top B_1+R \\ \star & -P_3-P_3^\top+\bar\eta^2 R & 0 & P_3^\top B_1 \\ \star & \star & -(S+R) & R \\ \star & \star & \star & -2R \end{pmatrix}, \tag{24}$$

where C, P, R, S, P_2 and P_3 are 2×2 matrices, and $\bar\eta$ is given by (18). Suppose that there exists $P>0$, $R\geq 0$, $S\geq 0$ and P_2, P_3 such that

$$Q(C_i;P,R,S,P_2,P_3)<0\,,\quad i=1,2,3\,, \tag{25}$$

with the matrices C_i given by (20) and $B_1=A_1$ defined by (14). Then, the trivial solution of the observer error-dynamics (17) is locally asymptotically stable.

Proof. The proof follows the descriptor approach [21], but we pay special attention to the nonlinear terms in (17) and incorporate the time-varying nature of the system. Consider again (22) and note that, for any $P_2, P_3\in\mathbb{R}^{2\times 2}$,

$$2\left(\varepsilon(\tau)^\top P_2^\top+\dot\varepsilon(\tau)^\top P_3^\top\right)\cdot\left(B_0(\tau)\varepsilon(\tau)+B_1\varepsilon(\tau-\eta(\tau))+H(\tau,\varepsilon(\tau))\varepsilon(\tau)-\dot\varepsilon(\tau)\right)=0$$

or, in matrix form,

$$E(\tau)^\top\begin{pmatrix} B_0(\tau)^\top P_2+P_2^\top B_0(\tau) & -P_2^\top+B_0(\tau)^\top P_3 & 0 & P_2^\top B_1 \\ \star & -P_3-P_3^\top & 0 & P_3^\top B_1 \\ \star & \star & 0 & 0 \\ \star & \star & \star & 0 \end{pmatrix}E(\tau)+2\left(\varepsilon(\tau)^\top P_2^\top+\dot\varepsilon(\tau)^\top P_3^\top\right)\cdot H(\tau,\varepsilon(\tau))\cdot\varepsilon(\tau)=0\,. \tag{26}$$

Observe that

$$2\left(\varepsilon(\tau)^\top P_2^\top+\dot\varepsilon(\tau)^\top P_3^\top\right)\cdot H(\tau,\varepsilon(\tau))\cdot\varepsilon(\tau)=\mathcal{O}(\|E(\tau)\|^3)\,,$$

so adding (26) to (23) gives

$$\dot V(\varepsilon_\tau)\leq -E^\top(\tau)Q(B_0(t);P,R,S,P_2,P_3)E(\tau)+\mathcal{O}(\|E(\tau)\|^3)\,.$$

Because of (19), there exists continuous real-valued functions c_i such that

$$B_0(\tau)=\sum_{i=1}^3 c_i(\tau)C_i\,,\quad c_i(\tau)\geq 0\,,\quad \sum_{i=1}^3 c_i(\tau)\equiv 1\,.$$

Since C appears affinely in (24), we have [21, Remark 3.6]

$$\dot V(\varepsilon_\tau)\leq -\sum_{i=1}^3 c_i(\tau)E^\top(\tau)Q(C_i;P,R,S,P_2,P_3)E(\tau)+\mathcal{O}(\|E(\tau)\|^3)\,.$$

By (25), the derivative of V is negative definite in a neighborhood of the origin and asymptotic stability follows. □

Perhaps not surprisingly, the LMI (25) is feasible if the delays are not too large. Allow us to formalize this statement.

Theorem 2. Let $\bar I<2\left(\sqrt{2}-1\right)$, and let the predictor gains satisfy

$$\alpha_2>\frac{\alpha_1^2+1}{a\alpha_1-1}\bar I\,,\quad \alpha_1>\frac{1}{a}\bar I\,,\quad a=\sqrt{4-4\bar I-\bar I^2}>0\,. \tag{27}$$

Then, the LMI (25) is feasible for $\bar\eta$ small enough.

Proof. Consider the case $\bar\eta=0$ and set $S=0$, $P_2=P$ and $P_3=\delta P$, where $\delta>0$ is a parameter to be determined later. The matrix Q (24) takes the form

$$Q(C;P,R,0,P,\delta P)=\begin{pmatrix} C^\top P+PC+R & \delta C^\top P & 0 & PB_1+R \\ \star & -2\delta P & 0 & \delta PB_1 \\ \star & \star & -R & R \\ \star & \star & \star & -2R \end{pmatrix}.$$

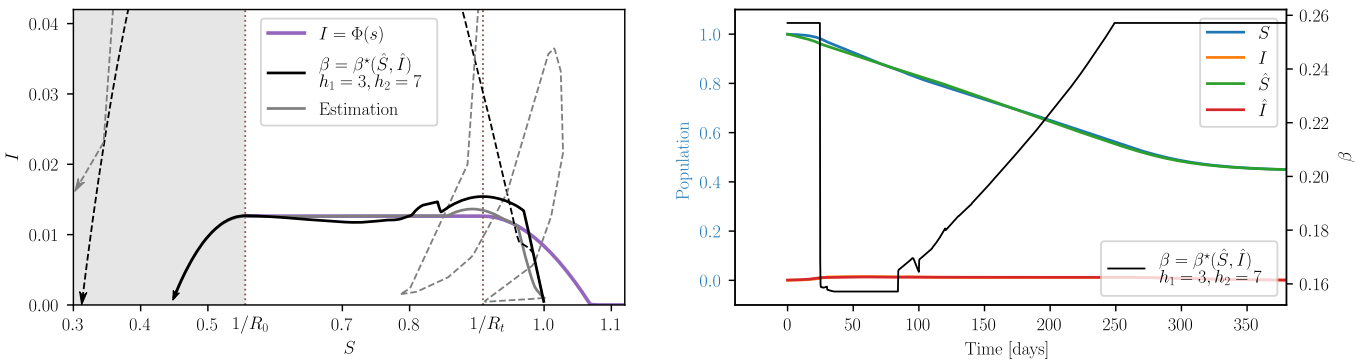

FIGURE 7 True and estimated trajectories under the feedback law $\beta = \beta^\star(\hat{S}, \hat{I})$, with $h_1 = 3$ and $h_2 = 7$ days (solid lines). For illustration purposes, we include the trajectories that correspond to an unstable prediction error (dashed lines).

By taking the Schur complement of Q with respect to the block

$$\begin{pmatrix} -R & R \\ \star & -2R \end{pmatrix},$$

we can readily see that the inequality $Q(C; P, R, 0, P, \delta P) < 0$ is equivalent to

$$\bar{Q}(C; P, R, \delta) = \begin{pmatrix} (C + B_1)^\top P + P(C + B_1) + PB_1R^{-1}B_1^\top P & \delta\left((C + B_1)^\top P + PB_1R^{-1}B_1^\top P\right) \\ \star & -2\delta P + \delta^2 PB_1R^{-1}B_1^\top P \end{pmatrix} < 0\,. \tag{28}$$

Take P as in (5). Direct computations show that (27) imply that

$$(C_i + B_1)^\top P + P(C_i + B_1) \leq -\bar{W}\,, \quad i = 1, \ldots, 3 \tag{29}$$

for some $\bar{W} > 0$. Let $\lambda_{\min}$ be the smallest eigenvalue of R. By (29), we can always choose R with λ_{min} large enough so that the upper-left block of $\bar{Q}$ is negative definite,

$$(C + B_1)^\top P + P(C + B_1) + PB_1R^{-1}B_1^\top P < 0\,.$$

For sufficiently small δ we have

$$-2\delta P + \delta^2 PB_1R^{-1}B_1^\top P < 0\,.$$

By taking now the Schur complement of $\bar{Q}$ with respect to its lower-right block we can see that, again for δ small enough, the LMI (28) is satisfied. We have shown that (25) is feasible for $\bar{\eta} = 0$. By continuity, it is also feasible for $\bar{\eta}$ small enough. □

For our example, we take a conservative approach and set

$$\bar{\eta} = 5 > (h_1 + h_2)\beta_{\max} = 2.4$$

and $\bar{I} = 30 \times 10^{-3}$ (recall that $I_{\max} = 12.63 \times 10^{-3}$). The gain $\alpha = \begin{pmatrix} 0.115 & 0.005 \end{pmatrix}$ lays within the intersection of the stability regions of p_1, p_2 and p_3.

The LMI (25) was solved using SCS[29]. A solution is

$$P = \begin{pmatrix} 51.1 & -140.6 \\ -140.6 & 979.2 \end{pmatrix}, \quad R = S = \begin{pmatrix} 16.3 & -0.6 \\ -0.6 & 3.3 \end{pmatrix} \quad \text{and} \quad P_2 = P_3 = \begin{pmatrix} 42.3 & -85.3 \\ -140.5 & 984.4 \end{pmatrix},$$

so, according to Thm. 1, the prediction error converges to zero asymptotically. This is illustrated in Fig. 7 (solid lines). The hospital capacity is now exceeded by 22 % (much smaller than the previous 200 %).

The correct tuning of the predictor parameters is, of course, critical. For illustration purposes, we consider the gain $\alpha = \begin{pmatrix} 1.03 & 0.04 \end{pmatrix}$, which lays outside the stability region described in Section 4. The response is also shown in Fig. 7 (dashed lines). The hospital capacity is now exceeded by more than 500 %.

6 | ON THE EFFECT OF MEASUREMENT ERRORS

A frequent situation in epidemics is poor output variable measurement, mainly due to underregistration. A sound assumption is that the output is proportional to the measured variable, $I(t-h_2)$. The proportion may be time-varying but always less than 1. It is described as

$$y(t) = I(t-h_2)m(t-h_2)$$

with

$$m(t) \in [1-\delta, 1] , \quad 0 \leq \delta < 1 . \tag{30}$$

The logarithmic term in the prediction error dynamics (10) is now

$$\ln\left(\frac{y(t-h_1)}{\hat{I}(t-h-h_1)}\right) = \ln\left(\frac{I(t-h)m(t-h)}{\hat{I}(t-h-h_1)}\right) = \ln\left(\frac{I(t-h)}{\hat{I}(t-h-h_1)}\right) + \ln(m(t-h)) .$$

Define $d(t) = \ln(m(t))$ and observe that, by (30), it satisfies $|d(t)| \leq \bar{d}$ with

$$\bar{d} = \ln\left(\frac{1}{1-\delta}\right) .$$

The prediction error now has the dynamics

$$\dot{\varepsilon}(\tau) = B_0(\tau)\varepsilon(\tau) + B_1\varepsilon(\tau-\eta(\tau)) + H(\tau,\varepsilon(\tau))\varepsilon(\tau) - \alpha d(\tau-\eta(\tau)) . \tag{31}$$

To analyze the effect of the measurement error on the system response, we compute the time derivative of the functional (22), now along the trajectories of system (31). Following the same steps as in the proof of Theorem 1, we obtain

$$\dot{V}(\varepsilon_\tau) \leq -\sum_{i=1}^{3} c_i(\tau)E^\top(\tau)Q(C_i; P, R, S, P_2, P_3)E(\tau) - 2\left(\varepsilon(\tau)^\top P_2^\top + \dot{\varepsilon}(\tau)^\top P_3^\top\right)\alpha d(\tau-\eta(\tau)) + \mathcal{O}(\|E(\tau)\|^3) .$$

From the order relation

$$2\left(\varepsilon(\tau)^\top P_2^\top + \dot{\varepsilon}(\tau)^\top P_3^\top\right)\alpha d(\tau-\eta(\tau)) = \mathcal{O}(\bar{d}\cdot\|E(\tau)\|)$$

we conclude that, for $\bar{d}$ small enough, the solutions are ultimately bounded with ultimate bound proportional to $\bar{d}$.

We now simulate the effects of the measurement noise described above. We take $\delta = 0.5$ and define $m(t)$ a random variable with a beta distribution. We perform simulations for the predictor and the observer (see Fig. 8). The measurement errors result in a higher number of infected people. The poor performance of the observer had already been established. Noise simply makes it worse. In the case of the predictor, the increment is relatively low if we take into account the high amplitude of the error.

7 | PREDICTION USING REAL DATA

Finally, we will evaluate the predictor's performance using real data from the covid epidemic in Mexico City. Figure 9 (top) shows records of active cases obtained on different days. Note that the number of active cases registered on the current day is quite unreliable but, as time goes by, the records are updated until further corrections become negligible. It can be seen that present data about cases that are older than 20 days is fairly accurate, so we take $h_2 = 20$.

We do not know the exact control strategy implemented by the public health officials, but we can use the community mobility to infer it. Indeed, it is reasonable to expect the transmission rate to be proportional to the mobility, so we set

$$\beta(t) = \beta_{\max}\cdot(1+\mathrm{chg}(t)) ,$$

where chg is the mobility change with respect to the baseline. Note that in this case we have $h_1 = 0$.

Following the guidelines of Section 4 with $h = h_1 + h_2 = 20$ we propose

$$\alpha_1 = 0.38 \quad \text{and} \quad \alpha_2 = 0.05 .$$

We activate the predictor at time $t = -h$ with an initial state defined by

$$\hat{S}(t) = 1 \quad \text{and} \quad \hat{I}(t) = I(t) , \quad t \in [-2h, -h] ,$$

where I is taken from the report available at day $t = 0$ (black line). The resulting prediction (dashed green line) closely matches the report that will appear 20 days later (solid green line). Consequently, the prediction $\hat{I}(0)$ is practically equal to the value that will be finally reported.

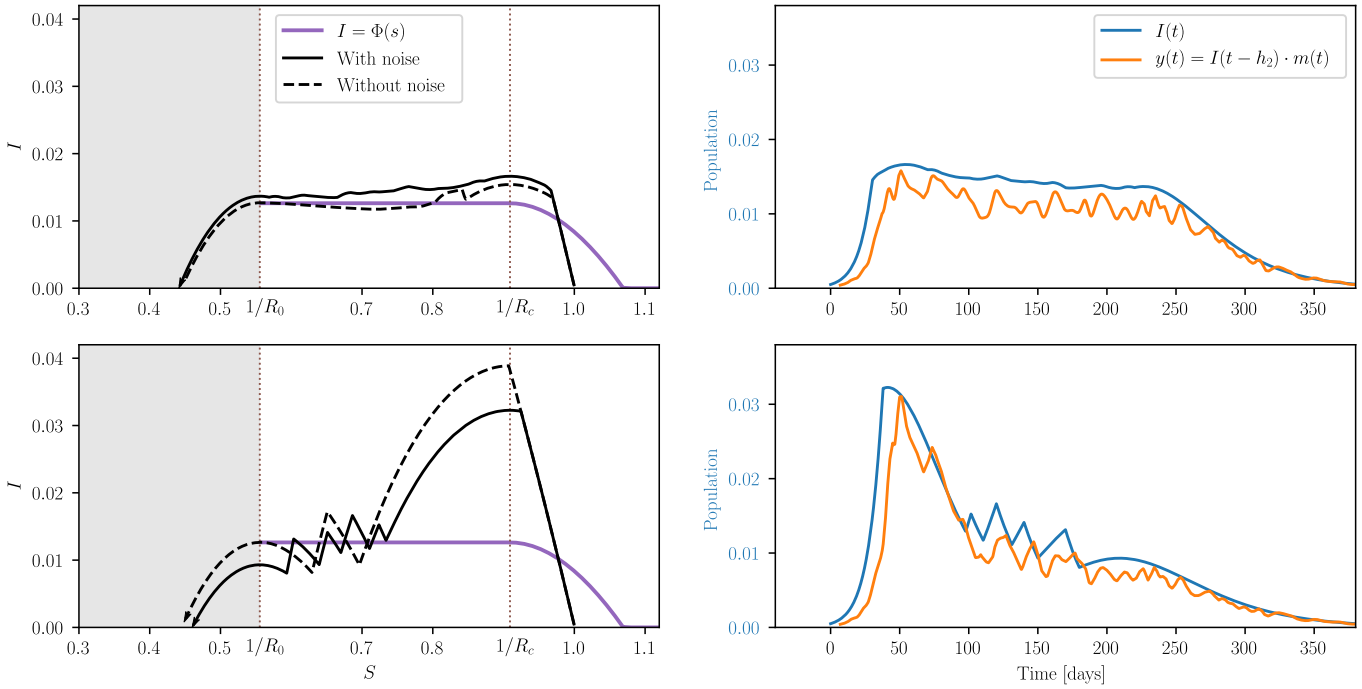

FIGURE 8 Closed-loop trajectories using the predictor (8) (top) and the observer (7) (bottom). Simulations were performed with and without measurement errors.

FIGURE 9 Prediction of the infected fraction of the population of Mexico City (dashed green line). The prediction is computed using records of active cases available at day zero[30] (black line, top), and of mobility changes[31] (black line, bottom). The prediction was obtained using (8) with $h_1 = 0$ and $h_2 = 20$. For comparison purposes, some future records of active cases are included. Day zero corresponds to August the 3rd, 2020.

8 | CONCLUSIONS

We have presented a predictor for systems with large input delays. The predictor is designed using the observer-predictor methodology introduced in the past years. In contrast with existing proposals, we present simple tuning criteria for ensuring the simultaneous stability of the polytopic model's vertices. The stability of the complete polytopic model is then established

formally with the help of a Lyapunov-Krasovskii functional. The functional can also be used to assess the sensitivity of the predictor with respect to error measurements. It is worthy of mentioning that it can also be used to find estimates of the domain of attraction, robustness bounds for the delay, and parameter uncertainties, among other problems of interest. The predictor was put to the test using real data from the covid pandemic in Mexico City, 2020. The results are encouraging and consistent with the analysis.

Our current research concerns the extension of the present results, obtained for two-dimensional systems, to *n*-dimensional ones, and to apply them to the study of more elaborated epidemic models involving states such as vaccinated individuals and asymptomatic ones.

References

1. Sharomi O, Malik T. Optimal control in epidemiology. *Annals of Operations Research* 2017; 251: 55–71.
2. Angulo MT, Castaños F, Velasco-Hernandez JX, Moreno JA. A simple criterion to design optimal nonpharmaceutical interventions for epidemic outbreaks. medRxiv eprint 2020.05.19.20107268; 2020.
3. Smith OJ. A controller to overcome dead time. *ISA J.* 1959; 6: 28–33.
4. Artstein Z. Linear systems with delayed controls: a reduction. *IEEE Transactions on Automatic control* 1982; 27(4): 869–879.
5. Manitius A, Olbrot A. Finite spectrum assignment problem for systems with delays. *IEEE Transactions on Automatic Control* 1979; 24(4): 541–552.
6. Bellman RE, Cooke KL. *Differential-difference equations*. New York: Academic Press . 1963.
7. Krstić M, Smyshlyaev A. *Boundary control of PDEs: A course on backstepping designs*. 16. SIAM . 2008.
8. Mondié S, Michiels W. Finite spectrum assignment of unstable time-delay systems with a safe implementation. *IEEE Transactions on Automatic Control* 2003; 48(12): 2207–2212.
9. Kharitonov VL. Predictor-based controls: the implementation problem. *Differential Equations* 2015; 51(13): 1675–1682.
10. Zhou B, Lin Z, Duan GR. Truncated predictor feedback for linear systems with long time-varying input delays. *Automatica* 2012; 48(10): 2387–2399.
11. Karafyllis I, Krstić M. Stabilization of nonlinear delay systems using approximate predictors and high-gain observers. *Automatica* 2013; 49(12): 3623 - 3631. doi: https://doi.org/10.1016/j.automatica.2013.09.006
12. Najafi M, Hosseinnia S, Sheikholeslam F, Karimadini M. Closed-loop control of dead time systems via sequential sub-predictors. *International Journal of Control* 2013; 86(4): 599–609.
13. Lechappe V, Moulay E, Plestan F. Prediction-based control for LTI systems with uncertain time-varying delays and partial state knowledge. *International Journal of Control* 2018; 91(6): 1403–1414. doi: 10.1080/00207179.2017.1317365
14. Germani A, Manes C, Pepe P. A new approach to state observation of nonlinear systems with delayed output. *IEEE Transactions on Automatic Control* 2002; 47(1): 96-101. doi: 10.1109/9.981726
15. Talebi S, Ataei M, Pepe P. An observer for a class of nonlinear systems with multiple state and measurement delays: A differential geometry-based approach. *European Journal of Control* 2020; 56: 132 - 141. doi: https://doi.org/10.1016/j.ejcon.2020.02.010
16. Zhou B, Liu Q, Mazenc F. Stabilization of linear systems with both input and state delays by observer-predictors. *Automatica* 2017; 83: 368–377. doi: https://doi.org/10.1016/j.automatica.2017.06.027
17. Estrada-Sánchez I, Velasco-Villa M, Rodríguez-Cortés H. Prediction-Based Control for Nonlinear Systems with Input Delay. *Mathematical Problems in Engineering* 2017(October): Article ID 7415418.

18. Neimark J. D-subdivisions and spaces of quasipolynomials. *Prikl., Mat. Meh* 1949; 13: 349–380.

19. Michiels W, Niculescu SI. *Stability and Stabilization of Time-Delay Systems*. SIAM . 2007

20. Gu K, Chen J, Kharitonov VL. *Stability of time-delay systems*. Springer Science & Business Media . 2003.

21. Fridman E. *Introduction to Time-Delay Systems, Analysis and Control*. Birkhäuser . 2014.

22. Boyd S, El Ghaoui L, Feron E, Balakrishnan V. *Linear Matrix Inequalities in System and Control Theory*. Philadelphia: Society for Industrial and Applied Mathematics . 1994.

23. He Y, Wu M, She JH, Liu GP. Parameter-dependent Lyapunov functional for stability of time-delay systems with polytopic-type uncertainties. *IEEE Transactions on Automatic control* 2004; 49(5): 828–832.

24. Batmani Y, Khaloozadeh H. On the Design of Observer for Nonlinear Time-Delay Systems. *Asian Journal of Control* 2014; 16(4): 1191-1201. doi: https://doi.org/10.1002/asjc.795

25. Yang R, Zhang G, Sun L. Observer-based finite-time robust control of nonlinear time-delay systems via Hamiltonian function method. *International Journal of Control* 2020; 0(0): 1-18. doi: 10.1080/00207179.2020.1774657

26. Aubin JP, Frankowska H. *Set-Valued Analysis*. Boston: Birkhäuser . 1990.

27. Capistran MA, Capella A, Christen JA. Forecasting hospital demand during COVID-19 pandemic outbreaks. arXiv eprint 2006.01873; 2020.

28. Khalil HK. *Nonlinear Systems*. Upper Saddle River, New Jersey: Prentice-Hall . 1996.

29. O'Donoghue B, Chu E, Parikh N, Boyd S. Conic Optimization via Operator Splitting and Homogeneous Self-Dual Embedding. *Journal of Optimization Theory and Applications* 2016; 169(3): 1042-1068.

30. Dirección General de Epidemiología, Datos Abiertos. https://www.gob.mx/salud/documentos/datos-abiertos-bases-historicas-direccion-general-de-epidemiologia; 2021-01-23.

31. Google COVID-19 Community Mobility Reports. https://www.google.com/covid19/mobility/; 2021-01-23.